

Double-Degradable Responsive Self-Assembled Multivalent Arrays – Temporary Nanoscale Recognition Between Dendrons and DNA

Anna Barnard,^a Paola Posocco,^b Maurizio Fermeglia,^b Ariane Tschiche,^c Marcelo Calderon,^c Sabrina Pricl,^{b,d} and David K. Smith^{*a}

a: Department of Chemistry, University of York, Heslington, York, YO10 5DD, UK

b: National Interuniversity Consortium for Material Science and Technology (INSTM), Research Unit MOSE-DEA, University of Trieste, 34127 Trieste, Italy

c: Institut für Chemie und Biochemie, Freie Universität Berlin, Takustrasse 3, D-14195 Berlin, Germany

d: Molecular Simulation Engineering (MOSE) Laboratory, Department of Engineering and Architecture (DEA), University of Trieste, 34127, Trieste, Italy

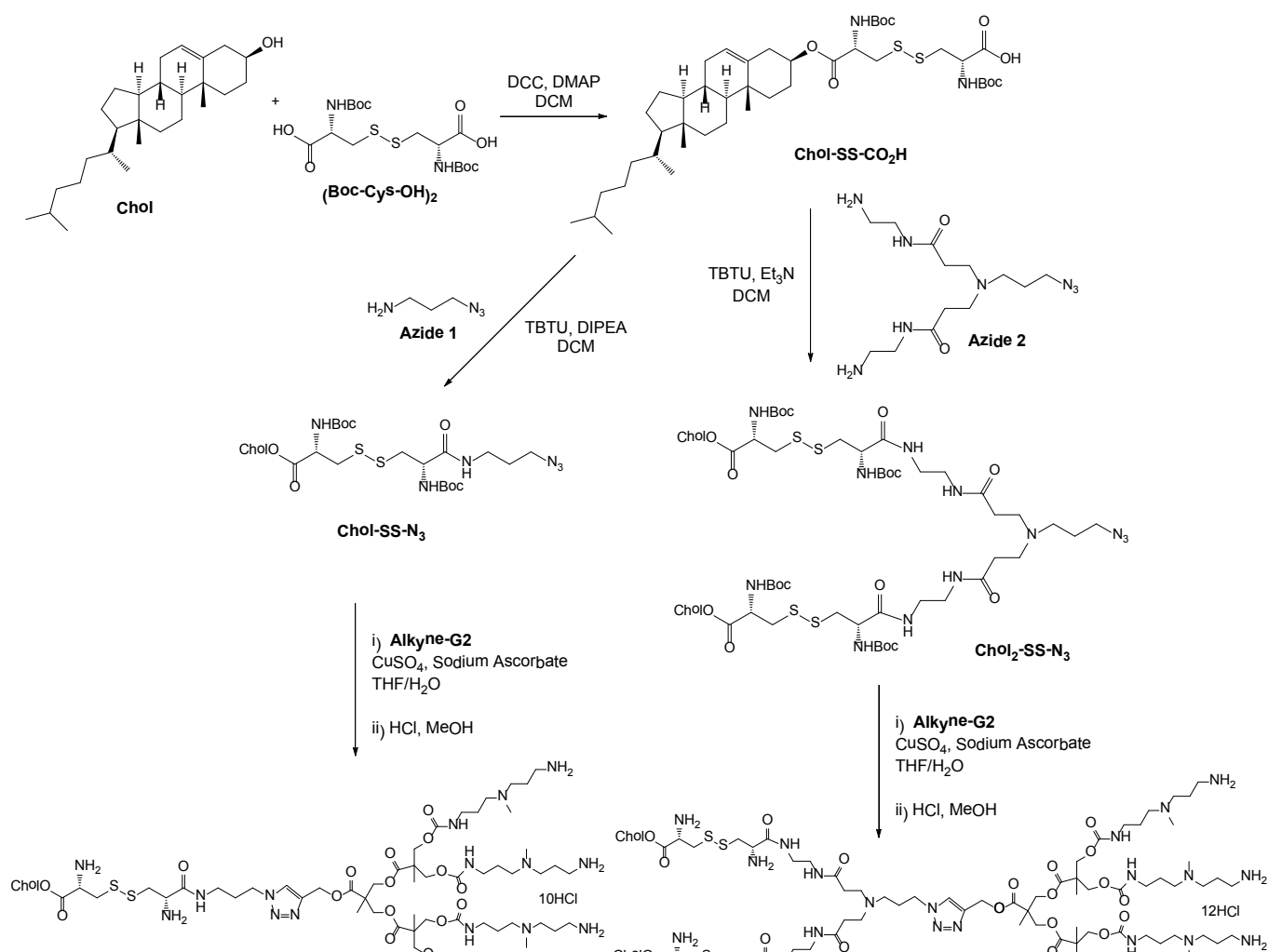
SUPPORTING INFORMATION

Contents

- 1 Synthesis and Characterisation of Dendrons
- 2 Self-Assembly Assays
- 3 DNA Binding Assays
- 4 Mass Spectrometric Assays
- 5 Degradation/DNA Release Assays
- 6 Multiscale Modelling Methods
- 7 References

1. Synthesis and Characterisation of Dendrons

1.1 Synthetic Scheme



1.2 General Materials and Methods

All reagents were obtained from commercial sources and were used without further purification. Azide functionalised linking groups (**Azide 1** and **Azide 2**) and alkyne-functionalised Fréchet-Hult dendrons (**Alkyne-G2**) were synthesised as described previously.^{1,2} Column chromatography was performed on silica gel 60 (35-70 μm) supplied by Fluka Ltd. Preparative gel permeation chromatography (GPC) was performed on Biobeads SX-1 supplied by Bio-Rad and Sephadex LH-20. Thin layer chromatography (TLC) was performed on Merck aluminium-backed plates, coated with 0.25 nm silica gel 60. ¹H, ¹³C, ¹H-¹H COSY and ¹H-¹³C HSQC NMR were recorded on either a JEOL ECX400 (¹H 400 MHz, ¹³C 100 MHz) spectrometer or a JEOL ECX270 (¹H 270 MHz, ¹³C 68 MHz). The high molecular weights of some

compounds meant in some cases quaternary carbon peaks could not be observed. ESI and HR-ESI mass spectra were recorded on a Bruker Daltonics Microtof mass spectrometer. Infrared spectra were recorded on a Shimadzu IRPrestige-21 FT-IR spectrometer.

1.3 Synthesis of Chol-SS-CO₂H

(**Boc-Cys-OH**)₂ (4.56 g, 10.4 mmol) was dissolved in DCM (50 ml) along with DMAP (1.70 g, 13.97 mmol) and DCC (3.2 g, 15.5 mmol). Cholesterol (**Chol**, 2.00 g, 5.2 mmol) dissolved in DCM (10 ml) was added dropwise over 1 h and the reaction mixture was stirred overnight at room temperature and then filtered through Celite. The solvent was removed *in vacuo* affording the crude product which was purified by column chromatography (SiO₂, 98:2 DCM: MeOH → 9:1 DCM: MeOH). The pure product was isolated as an off-white foam (1.8 g, 2.2 mmol, 43%). *R_f* = 0.43 (9:1 DCM: MeOH). ¹H NMR (400 MHz, CDCl₃) δ: 5.36 (s, CH_A, 1H); 4.64-4.47 (m, CH_B, CHNHBoc, 3H); 3.56-3.14 (br m, CH₂S, 4H); 2.31 (s, CH₂CH_B, 2H); 1.98-1.83 (m, CH and CH₂ cholesterol, 5H); 1.58-0.84 (m, CH, CH₂ and CH₃ cholesterol, C(CH₃)₃, 51H); 0.66 (s, CH₃ cholesterol, 3H). ¹³C NMR (100 MHz, CDCl₃) δ: 170.31 (C=O); 155.44 (CONH); 155.35 (CONH); 139.39 (CCH_A); 123.06 (CH_A); 80.33 (C(CH₃)₃); 75.66 (CH_B); 56.76, 56.23 (CH cholesterol); 53.51 (CHNHBoc); 50.07, 42.39 (CH cholesterol); 39.80, 39.59, 37.96, 36.99, 36.63, 36.29 (CH₂ cholesterol, CH₂S); 35.89 (CH cholesterol); 31.91 (CH₂ cholesterol); 28.46 (C(CH₃)₃); 28.09, 27.72, 24.37, 23.94 (CH₂ cholesterol); 22.91, 22.65 (CH cholesterol); 21.12 (CH₂ cholesterol); 19.41, 18.81, 11.95 (CH₃ cholesterol). ESI-MS: 809.48 [M+H]⁺ (20%); 831.46 [M+Na] (100%). HRMS: Calcd. [M+H]⁺ (C₄₃H₇₃N₂O₈S₂) *m/z* = 809.4803. Found [M+H]⁺ *m/z* = 809.4779. *v*_{max} (cm⁻¹): 3340br w (O-H), 2932s (C-H), 1713s (C=O), 1356m, 1250w, 1165m, 1018w, 856w, 772w. [α]_D = -5.4 (c. 1.0, CHCl₃).

1.4 Synthesis of Chol-SS-N₃

Chol-SS-CO₂H (200 mg, 0.25 mmol) was dissolved in DCM (20 ml) along with **Azide 1**¹ (67 mg, 0.5 mmol) and DIPEA (171 μl, 0.99 mmol). TBTU (159 mg, 0.5 mmol) was then added and the reaction mixture was stirred overnight at room temperature. The solvent was removed *in vacuo* and the crude product purified by column chromatography (SiO₂, 97:3 DCM: MeOH) affording the pure product as a white foam (213 mg, 0.24 mmol, 97%). *R_f* = 0.59 (97:3 DCM: MeOH). ¹H NMR (400 MHz, CDCl₃) δ: 5.55 (s, CH_A, 1H); 4.64-4.41 (m, CH_B, CHNHBoc, 3H); 3.33-3.04 (m, CH₂S, CH₂NH, CH₂N₃, 8H); 2.31 (s, CH₂CH_B, 2H); 1.99-1.76 (m, CH and CH₂ cholesterol, CH₂CH₂NH, 7H); 1.64-0.81 (m, CH, CH₂ and CH₃ cholesterol, C(CH₃)₃, 51H); 0.64 (s, CH₃ cholesterol, 3H). ¹³C NMR (100 MHz, CDCl₃) δ: 170.69 (C=O); 155.40 (CONH); 155.32 (CONH); 139.25 (CCH_A); 123.11 (CH_A); 80.35 (C(CH₃)₃); 75.87

(CH_B); 56.72, 56.17 (CH cholesterol); 53.42 (CHNHBoc); 50.04 (CH cholesterol); 49.14 (CH₂N₃); 42.35 (CH cholesterol); 39.76, 37.99 (CH₂ cholesterol); 37.15 (CH₂NH); 36.94, 36.61, 36.23 (CH₂ cholesterol, CH₂S); 35.84 (CH cholesterol); 31.95 (CH₂ cholesterol); 28.71 (CH₂CH₂NH); 28.40 (C(CH₃)₃); 28.06, 27.70, 24.34, 23.88 (CH₂ cholesterol); 22.91, 22.64 (CH and CH₃ cholesterol); 21.08 (CH₂ cholesterol); 19.37, 18.79, 11.92 (CH₃ cholesterol). ESI-MS: 891.54 [M+H]⁺ (30%), 913.52 [M+Na]⁺ (100%). HRMS: Calcd. [M+H]⁺ (C₄₆H₇₉N₆O₇S₂) *m/z* = 891.5446. Found [M+H]⁺ *m/z* = 891.5427. *v*_{max} (cm⁻¹): 3310*m* (N-H), 2932*s* (C-H), 2099*s* (N₃), 1705*s* (C=O ester), 1667*s* (C=O amide), 1504*s*, 1366*w*, 1250*m*, 1165*s*, 1018*m*, 864*w*, 779*w*, 625*w*. [α]_D = -3.0 (c. 0.5, CHCl₃).

1.5 Synthesis of Chol₂-SS-N₃

Chol-SS-CO₂H (210 mg, 0.26 mmol) was dissolved in DCM (40 ml) along with **Azide 2¹** (21.3 mg, 0.065 mmol) and triethylamine (72 μl, 0.52 mmol). TBTU (83 mg, 0.26 mmol) was then added and the reaction mixture was stirred overnight at room temperature. The solution was washed with HCl (2 x 30 ml, 1M), Na₂CO₃ (2 x 30 ml, 1M) and H₂O (30 ml). The organic phase was dried over MgSO₄, filtered and the filtrate evaporated *in vacuo* affording the crude product as a pale yellow foam. The crude product was purified by column chromatography (SiO₂, 95:5 DCM: MeOH) affording the pure product as an off-white sticky solid in moderate yield (51 mg, 0.027 mmol, 28%). *R*_f = 0.67 (95:5 DCM: MeOH). ¹H NMR (400 MHz, CDCl₃) δ: 7.31 (br s, NH, 4H); 5.62 (br s NH, 4H); 5.36 (s, CH_A, 2H); 4.66-4.42 (m, CH_B, CHNHBoc, 6H); 3.36-2.96 (m, CH₂N₃, CH₂S, CH₂NH, 18H); 2.67 (br s, C(O)CH₂, 4H); 2.47 (s, CH₂CH_B, 4H); 2.33 (s, N(CH₂)₃, 6H); 2.00-0.83 (m, CH, CH₂ and CH₃ cholesterol, CH₂CH₂NH, C(CH₃)₃, 114H); 0.66 (s, CH₃ cholesterol, 6H). ¹³C NMR (100 MHz, CDCl₃); δ: 173.19 (C=O); 155.27 (CONH); 139.20 (CCH_A); 123.00 (CH_A); 80.23 (C(CH₃)₃); 75.74 (CH_B); 56.62, 56.08 (CH cholesterol); 53.37 (CHNHBoc); 49.94 (N(CH₂)₃); 49.10 (CH₂N₃); 42.26, 39.66, 39.47, 37.90, 36.84, 36.52, 36.13, 35.74, 31.78 (CH, CH₂ cholesterol, CH₂S, CH₂NH, C(O)CH₂); 28.33 (C(CH₃)₃); 28.18, 27.97, 27.62, 25.74, 24.24, 23.78 (CH₂CH₂N₃, CH₂ cholesterol); 22.78, 22.52 (CH and CH₃ cholesterol); 20.98 (CH₂ cholesterol); 19.27, 18.67, 11.81 (CH₃ cholesterol). ESI-MS: 1911.2 [M+H]⁺ (100%). HRMS: Calcd. [M+H]⁺ (C₉₉H₁₇₀N₁₂O₁₆S₄) *m/z* = 1911.1735. Found [M+H]⁺ *m/z* = 1911.1713. *v*_{max} (cm⁻¹): 3302*m* (N-H), 2932*m* (C-H), 2099*m* (N₃), 1697*s* (C=O), 1659*s* (C=O), 1504*m*, 1366*m*, 1242*m*, 1157*s*, 1018*w*, 864*w*, 733*w*. [α]_D = 6.0 (c. 0.5, CHCl₃).

1.6 Synthesis of Chol-SS-G2(Boc)

Alkyne-G2² (212 mg, 142 μmol) was dissolved in degassed THF:H₂O (5 ml, 1:1). **Chol-SS-N₃** (115 mg, 130 μmol) dissolved in degassed THF: H₂O (5 ml, 1:1) was then added along with CuSO₄.5H₂O (3.2 mg,

13 μmol , 10 mol%) and sodium ascorbate (5.1 mg, 26 μmol , 20 mol%). The reaction mixture was stirred overnight at room temperature. The THF was then removed *in vacuo* at room temperature and the residue taken up in DCM (20 ml). The solution was washed with H_2O (2 x 10 ml). The organic phase was dried over MgSO_4 , filtered and the filtrate evaporated *in vacuo*. The crude product was purified by GPC (DCM) affording the pure product as an off-white foam (174 mg, 73 μmol , 56%). $R_f = 0.97$ (95:5, MeOH: NH_4OH). ^1H NMR (400 MHz, CDCl_3) δ : 7.84 (br s, CH triazole, 1H); 6.07 (br s, NH, 4H); 5.40-5.20 (m, CH_A , NH, 8H); 4.40-4.01 (m, CH_B , CH_2O , CHNHBoc , 17H); 3.15-3.09 (m, CH_2N triazole, CH_2NH , CH_2S , 24H); 2.34-2.33 (m, $\text{CH}_2\text{N}(\text{CH}_3)$, 16H); 2.13 (s, $\text{N}(\text{CH}_3)$, 12H); 1.94-0.80 (m, $\text{CH}_2\text{CH}_2\text{NH}$, $\text{C}(\text{CH}_3)_3$, $\text{CH}_3\text{C}(\text{CH}_2\text{O})_2$, CH, CH_2 , CH_3 cholesterol, 121H); 0.62 (s, CH_3 cholesterol, 3H). ^{13}C NMR (100MHz, CDCl_3) δ : 172.29 (C=O); 156.03 (CONH); 155.98 (CONH); 141.70 (C triazole); 139.09 (C CH_A); 124.91 (CH triazole); 122.90 (CH_A); 78.67 ($\text{C}(\text{CH}_3)_3$); 75.63 (CH_B); 65.67-65.04 (CH_2O); 56.52, 55.98 (CH cholesterol); 55.62 (CH_2 triazole); 53.34 (CHNHBoc); 49.85 (CH cholesterol); 46.95 (quaternary C); 42.16 (quaternary C cholesterol); 41.66 (NCH_3); 39.71, 39.36, 39.19, 37.80, 36.74, 36.42, 36.03, 35.63, 31.69 (CH, CH_2 cholesterol, CH_2S , CH_2NH); 28.34 ($\text{C}(\text{CH}_3)_3$); 28.08 ($\text{CH}_2\text{CH}_2\text{NH}$); 27.86, 27.10, 26.70, 24.14, 23.67, 22.69 (CH_2 cholesterol); 22.43 (CH and CH_3 cholesterol); 20.88 (CH_2 cholesterol); 19.17, 18.58 (CH_3 cholesterol); 17.30 (CH_3); 11.72 (CH_3 cholesterol). ESI-MS: 794.5 [$\text{M}+3\text{H}$] $^{3+}$ (100%), 1190.2 [$\text{M}+2\text{H}$] $^{2+}$ (20%). HRMS: Calcd. [$\text{M}+2\text{H}$] $^{2+}$ ($\text{C}_{116}\text{H}_{208}\text{N}_{18}\text{O}_{29}\text{S}_2$) $m/z = 1190.7393$. Found [$\text{M}+2\text{H}$] $^{2+}$ $m/z = 1190.7384$. ν_{max} (cm^{-1}): 3325 m (N-H), 2940 m (C-H), 1690 s (C=O), 1520 s , 1458 m , 1365 m , 1242 s , 1126 s , 1026 m , 918 w , 864 w , 771 w , 733 w . $[\alpha]_D = 3.8$ (c. 0.5, CHCl_3).

1.7 Synthesis of Chol-SS-G2

Chol-SS-G2(Boc) (178 mg, 75 μmol) was dissolved in MeOH (20 ml) and HCl gas was bubbled through the solution for 20 s. The reaction mixture was stirred at room temperature for 3 h. The solvent was removed *in vacuo* affording the product as an off-white sticky solid (161 mg, 75 μmol , 100%). $R_f = 0.00$ (NH_4OH). ^1H NMR (400MHz, MeOD) δ : 8.07 (br s, CH triazole, 1H); 5.37 (m, CH_A , 1H); 4.43-4.09 (m, CH_B , CH_2O , CHNH_2 , 17H); 3.27-2.93 (m, CH_2N triazole, CH_2NH , CH_2NH_2 , CH_2S , 24H); 2.39-2.23 (m, $\text{CH}_2\text{N}(\text{CH}_3)$, 16H); 2.01 (br s, $\text{N}(\text{CH}_3)$, 12H); 1.83-0.82 (m, $\text{CH}_2\text{CH}_2\text{NH}$, $\text{CH}_3\text{C}(\text{CH}_2\text{O})_2$, CH, CH_2 , CH_3 cholesterol, 67H); 0.67 (s, CH_3 cholesterol, 3H). ^{13}C NMR (100MHz, MeOD) δ : 172.77 (C=O); 157.03 (CONH); 139.22 (C triazole); 138.97 (C CH_A); 122.92 (CH_A); 65.76 (CH_2O); 56.76, 56.23 (CH cholesterol); 54.31 (CH_2 triazole); 53.69 (CHNH_2); 53.15, 52.12, 50.19 (CH cholesterol); 46.63 (quaternary C); 42.18 (quaternary C cholesterol); 39.72, 39.36, 37.96, 37.83, 37.00, 36.80, 36.44, 36.06, 35.79, 31.85, 31.72 (NCH_3 , CH, CH_2 cholesterol, CH_2S , CH_2NH); 28.01 ($\text{CH}_2\text{CH}_2\text{NH}$); 27.82, 24.65, 24.01, 23.62, 22.30 (CH_2 cholesterol); 21.93, 21.68 (CH and CH_3 cholesterol); 20.84 (CH_2 cholesterol);

18.53, 17.99 (CH₃ cholesterol); 17.05 (CH₃); 11.07 (CH₃ cholesterol). ESI-MS: 446.0 [M+4H]⁴⁺ (80%), 594.3 [M+3H]³⁺ (100%). HRMS: Calcd. [M+3H]³⁺ (C₈₆H₁₆₁N₁₈O₁₇S₂) *m/z* = 594.0571. Found [M+3H]³⁺ *m/z* = 594.0554. *v*_{max} (cm⁻¹): 3364*m* (N-H), 2940*m* (C-H), 1697*s* (C=O), 1528*m*, 1466*m*, 1250*s*, 1134*m*, 1026*w*, 525*s*. [α]_D = -3.4 (c. 0.5, MeOH).

1.8 Synthesis of Chol₂-SS-G2(Boc)

Alkyne-G2² (140 mg, 94 μmol) was dissolved in degassed THF: H₂O (5 ml, 1:1). **Chol₂-SS-N₃** (163 mg, 85 μmol) dissolved in degassed THF: H₂O (5 ml, 1:1) was then added along with CuSO₄·5H₂O (2.4 mg, 9.4 μmol, 10 mol%) and sodium ascorbate (3.7 mg, 18.8 μmol, 20 mol%). The reaction mixture was stirred overnight at room temperature. The THF was then removed *in vacuo* at room temperature and the residue taken up in DCM (20 ml). The solution was washed with H₂O (2 x 10 ml). The organic phase was dried over MgSO₄, filtered and the filtrate evaporated *in vacuo*. The crude product was purified by GPC (DCM) affording the pure product as an off-white foam (158.2 mg, 46.5 μmol, 55%). *R*_f = 0.42 (98:2 MeOH: NH₄OH). ¹H NMR (400 MHz, CDCl₃) δ: 7.84 (br s, CH triazole, 1H); 7.45 (br s, NH, 2H); 6.08 (br s, NH, 4H); 5.41 (br s, NH, 6H); 5.20 (br s, CH_A, 2H); 4.61-4.03 (m, CH_B, CHNH₂Boc, CH₂O, 20H); 3.31-3.09 (m, CH₂N triazole, CH₂NH, CH₂S, 34H); 2.61-2.28 (m, C(O)CH₂, CH₂CH_B, N(CH₂)₃, CH₂N(CH₃), 30H); 2.13 (s, N(CH₃), 12H); 1.94-0.80 (m, CH₂CH₂NH, C(CH₃)₃, CH₃C(CH₂O)₂, CH, CH₂, CH₃ cholesterol, 175H); 0.62 (s, CH₃ cholesterol, 6H). ¹³C NMR (100 MHz, CDCl₃) δ: 172.77 (C=O); 169.98 (C=O); 156.04 (CONH); 139.12 (CCH_A); 124.78 (CH triazole); 123.03 (CH_A); 80.16 (C(CH₃)₃); 78.86 (C(CH₃)₃); 75.68 (CH_B); 65.76 (CH₂O); 56.71, 56.17 (CH cholesterol); 55.78 (CH₂N triazole); 53.53 (CHNH₂Boc); 50.02 (N(CH₂)₃); 47.14 (quaternary C); 42.34, 41.85, 39.89, 39.36, 37.98, 36.93, 36.60, 36.22, 35.82, 31.87 (CH, CH₂ cholesterol, CH₂S, CH₂NH, N(CH₃), C(O)CH₂); 28.52 (C(CH₃)₃); 28.43 (C(CH₃)₃); 28.04, 27.28, 26.87, 24.32, 23.86 (CH₂CH₂NH, CH₂ cholesterol); 22.88, 22.62 (CH and CH₃ cholesterol); 21.07 (CH₂ cholesterol); 19.36, 18.76, 11.90 (CH₃ cholesterol). ESI-MS: 1134.4 [M+3H]³⁺ (100%), 1701.0 [M+2H]²⁺ HRMS: Calcd. [M+3H]³⁺ (C₁₆₉H₂₉₉N₂₄O₃₈S₄) *m/z* = 1133.7023. Found [M+3H]³⁺ *m/z* = 1133.6994. *v*_{max} (cm⁻¹): 3318*br m* (N-H); 2940*m* (C-H); 1697*s* (C=O); 1520*s*, 1458*m*, 1366*m*, 1250*s*, 1165*m*, 1018*m*, 795*m*, 532*m*. [α]_D = -8.2 (c. 0.5, MeOH).

1.9 Synthesis of Chol₂-SS-G2

Chol₂-SS-G2(Boc) (158 mg, 46.5 μmol) was dissolved in MeOH (20 ml) and HCl gas was bubbled through the solution for 20 s. The reaction mixture was stirred at room temperature for 3 h. The solvent was removed *in vacuo* affording the product as an off-white sticky solid (139 mg, 46 μmol, 99%). *R*_f = 0.00 (NH₄OH). ¹H NMR (400MHz, MeOD: CDCl₃, 8:2) δ: 7.99 (br s, CH triazole, 1H); 5.20 (br s, CH_A,

2H); 4.48-3.88 (br m, CH_B , $CHNH_2$, CH_2 , 20H); 3.30-2.69 (br m, CH_2N triazole, CH_2NH , CH_2S , 34H); 2.17-2.03 (m, $C(O)CH_2$, CH_2CH_B , $N(CH_2)_3$, $CH_2N(CH_3)$, 30H); 1.79 (s, $N(CH_3)$, 12H); 1.35-0.62 (m, CH_2CH_2NH , $C(CH_3)_3$, $CH_3C(CH_2O)_2$, CH , CH_2 , CH_3 cholesterol, 103H); 0.46 (s, CH_3 cholesterol, 6H). ^{13}C NMR (100MHz, MeOD: $CDCl_3$, 8:2) δ : 173.69 ($C=O$); 168.02 ($C=O$); 157.82 ($CONH$); 139.92 (CCH_A); 124.05 (CH triazole); 70.72 (CH_B); 65.68 (CH_2O); 56.75, 56.27 (CH cholesterol); 54.10 (CH_2N triazole); 53.06 ($CHNH_2$); 52.17 (CH cholesterol); 50.12 ($N(CH_2)_3$); 47.02 (quaternary C); 42.28, 39.74, 39.46, 37.70, 36.92, 36.52, 36.17, 35.85, 31.85 (CH , CH_2 cholesterol, CH_2S , CH_2NH , $N(CH_3)$, $C(O)CH_2$); 28.16, 27.90, 27.43, 24.51, 23.82 (CH_2CH_2NH , CH_2 cholesterol); 22.35, 22.09 (CH and CH_3 cholesterol); 21.00 (CH_2 cholesterol); 18.92, 18.39 (CH_3 cholesterol); 17.11 (CH_3); 11.53 (CH_3 cholesterol). ESI-MS: 650.6 $[M+4H]^{4+}$ (100%), 867.1 $[M+3H]^{3+}$ (20%). HRMS: Calcd. $[M+3H]^{3+}$ ($C_{129}H_{235}N_{24}O_{22}S_4$) $m/z = 866.8958$. Found $[M+3H]^{3+}$ $m/z = 866.8905$. ν_{max} (cm^{-1}): 3356w (N-H); 2940m, (C-H); 1713s ($C=O$); 1535m, 1466m, 1242s, 1134m, 1026m, 733m. $[\alpha]_D = -24$ (c. 0.5, $CHCl_3$: MeOH, 1:1).

2 Self-Assembly Assays

2.1 Nile Red Encapsulation³

A 2.5 mM Nile Red stock solution was made in EtOH. A dendron stock solution was made up in PBS buffer at various concentrations depending on the starting concentration for the assay. Aliquots of the stock solution were taken and diluted with PBS to the desired concentration in a 1 ml assay volume. Nile red (1 μ l) was added and the fluorescence emission was measured on a Hitachi F-4500 spectrofluorimeter using an excitation wavelength of 550 nm. Fluorescence intensity was recorded at 635 nm. Experiments were performed in triplicate.

2.2 Transmission Electron Microscopy

10 μ l of sample solution, in H_2O , was placed on a standard copper grid with Formvar and a carbon support film and allowed to set for three minutes. The grid was then stained with uranyl acetate (1% in water, pH 4.5). The grids were allowed to rest for ten minutes before being imaged. Imaging was performed on a FEI Technai 12 Biotwin operated at 120 kV.

2.3 Zeta Sizing

Zeta sizing measurements were carried out by Ariane Tschiche and Marcelo Calderon at Freie Universität Berlin. Dendron solutions were freshly prepared in HEPES buffer (2 mM HEPES, 9.4 mM NaCl) at pH 7.4 either alone (1 mg/ml) or complexed with a short DNA sequence (5'-CTGGACTTCCAGAAGAACATT-3') at the appropriate N:P ratio. The samples were incubated at room temperature for 30 minutes and stirred to ensure even distribution. Zeta potential was measured by applying an electric field across the solutions using laser Doppler anemometry on a Zetasizer Nano ZS analyser with an integrated 4 mW He-Ne laser at 633 nm. All measurements were carried out at 25 °C using folded capillary cells (DTS 1060). Measurements were carried out on a Zetasizer Nano (Malvern Instruments Ltd.) The autocorrelation functions were analysed using DTS v5.1 software provided by Malvern. Measurements were done in triplicate with 15–20 runs per single measurement and the calculated mean values (based in volume distribution) were used.

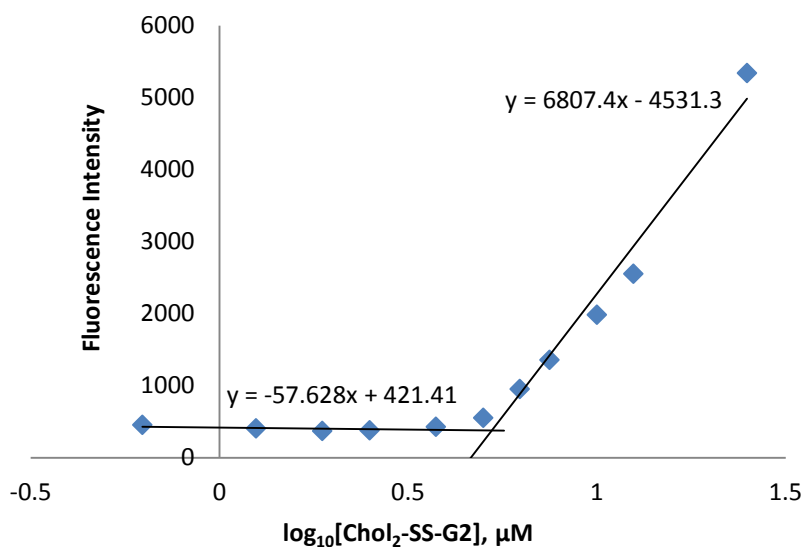
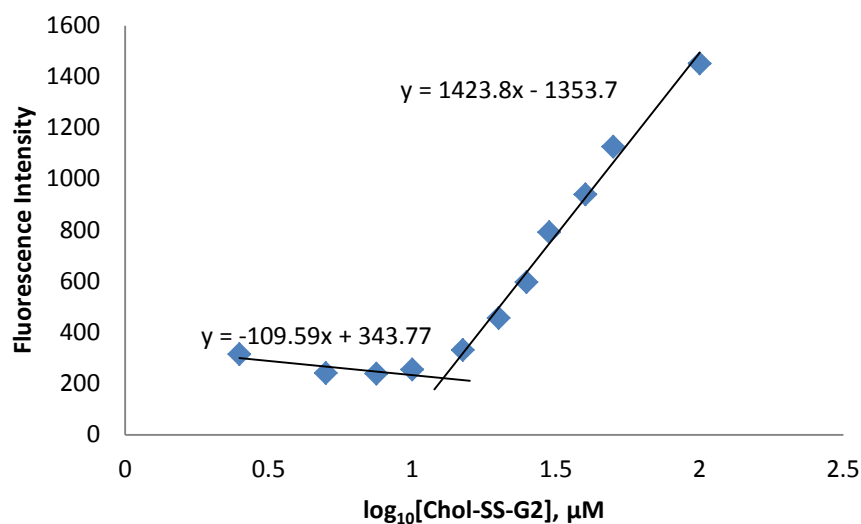


Figure S1. Graphs of \log_{10} of the concentration of Chol-SS-G2 (upper graph) and Chol₂-SS-G2 (lower graph) versus fluorescence intensity (635 nm) used to determine the C.A.C.

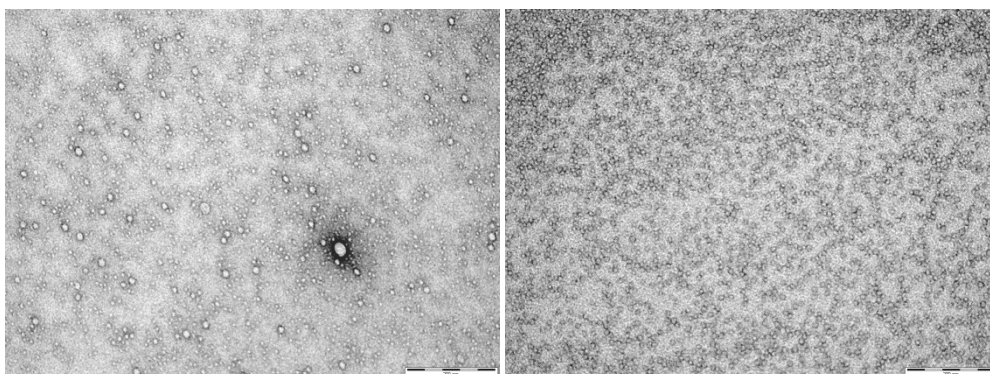


Figure S2. TEM images of Chol-SS-G2 (left) and Chol₂-SS-G2(right), scale bars = 200 nm.

3 DNA Binding Assays

3.1 Ethidium Bromide Displacement⁴

A solution of Calf Thymus DNA (8.0 μM) was prepared in SHE Buffer (2 mM HEPES, 0.05 mM EDTA, 150mM NaCl) at pH 7.5. Ethidium bromide was diluted with SHE Buffer to give a final concentration of 10.14 μM . Background ethidium bromide fluorescence was measured at 5.07 μM . The dendron stock solution, at varying concentration depending on the charge of the dendron, was prepared in a 50:50 solution of the ethidium bromide and DNA solutions to give a final EthBr concentration of 5.07 μM and DNA at 4.0 μM with respect to one DNA base (M_r 330 g mol^{-1}). Appropriate amounts of the dendron solution were added to 2 ml of a stock containing EthBr (5.07 μM) and DNA (4.0 μM) to achieve the desired N:P ratio. The fluorescence was measured on a Hitachi F-4500 spectrofluorimeter using an excitation wavelength of 540 nm. Fluorescence intensity was recorded at 595 nm. The fluorescence values were normalised to a solution containing only DNA (4.0 μM) and EthBr (5.07 μM). Experiments were performed in triplicate.

3.2 Gel Retardation

A solution of DNA (pGL3 plasmids, 1 mg/ml) was prepared in PIPES buffer (20 mM PIPES, 150 mM NaCl) at pH 7.5. Varying amounts of dendron dissolved in buffer were added to make up the solutions to the desired weight ratio. The solutions were each mixed with 2 μl of loading dye. 15 μl of each solution was then run in a 1% agarose gel (1 $\mu\text{l}/20\text{ml}$ ethidium bromide) for 30 minutes at 120V.

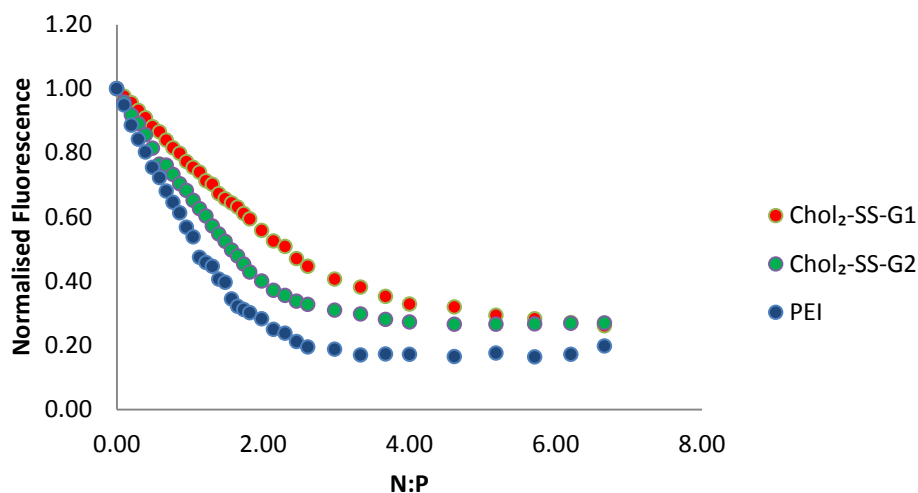


Figure S3. N:P ratio versus normalised fluorescence from the EthBr assay used to determine CE_{50} values.

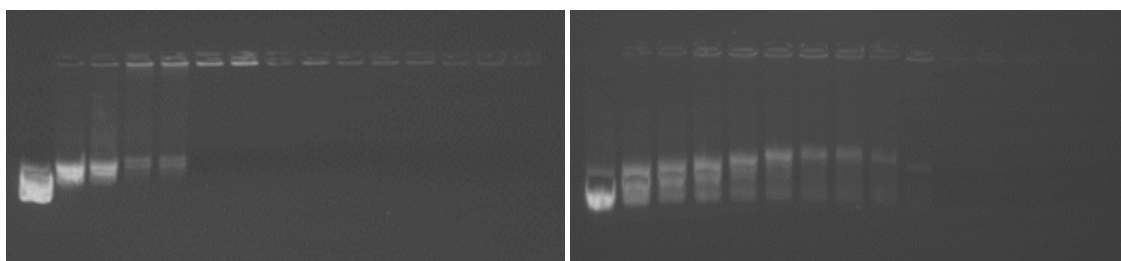


Figure S4 Gel electrophoresis images of pGL3 plasmid DNA (left hand lane). Increasing quantities of dendron (left to right) – lanes 2-15 (0.25:1 dendron: DNA, 0.5:1, 0.75:1, 1:1, 1.25:1, 1.5:1, 1.75:1, 2:1, 2.25:1, 2.5:1, 2.75:1, 3:1, 3.5:1, 4:1). Left = **Chol-SS-G2**; Right = **Chol₂-SS-G2**.

4 Mass Spectrometric Assays¹

Dendron solutions were prepared in either 10 mM ammonium acetate buffer (pH 5.0) or 10 mM ammonium carbonate buffer (pH 7.5) at a concentration of 200 μ M. 250 μ l aliquots of the dendron solution were removed periodically and combined with 250 μ l of a standard solution containing the dipeptide Gly-Ala (1 mM). The molecular weight was determined periodically by mass spectrometry with 100 μ M solutions of the dendron. Mass spectra were recorded in positive ion mode on a Bruker Esquire 6000 3D Ion-Trap electrospray mass spectrometer. Samples were injected at 240 μ l/hr, nebulizer pressure was 10.0 psi, dry gas temperature was 300°C and in Smart Parameter Setting Mode the Compound Stability was set to 30%. Experiments were performed in triplicate.

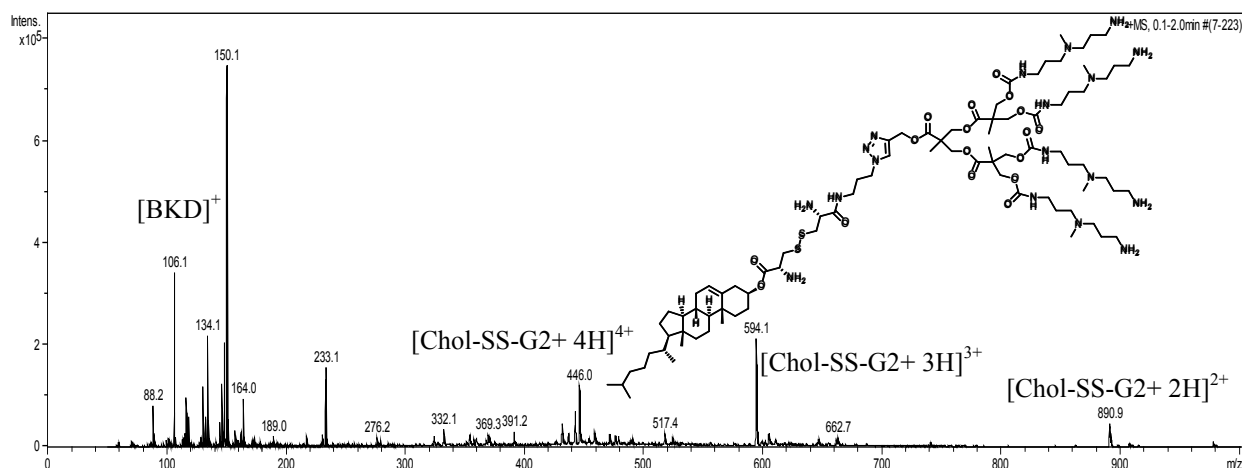


Figure S5. Mass spectra at time = 0 h, for Chol-SS-G2.

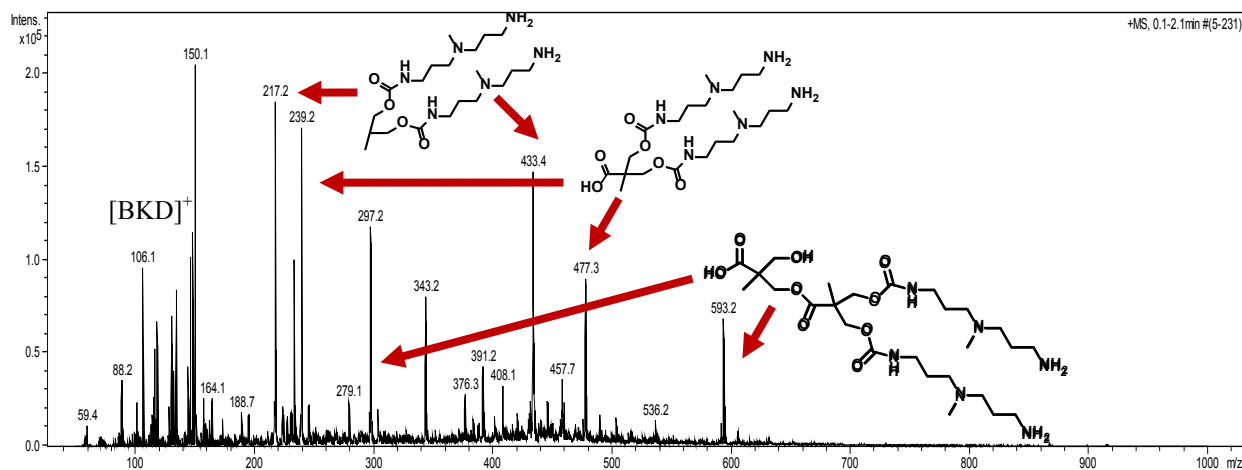


Figure S6. Mass spectra at time = 24 h for Chol-SS-G2 after stirring at pH 7.5 at 37°C. The structure of some of the degradation products are illustrated.

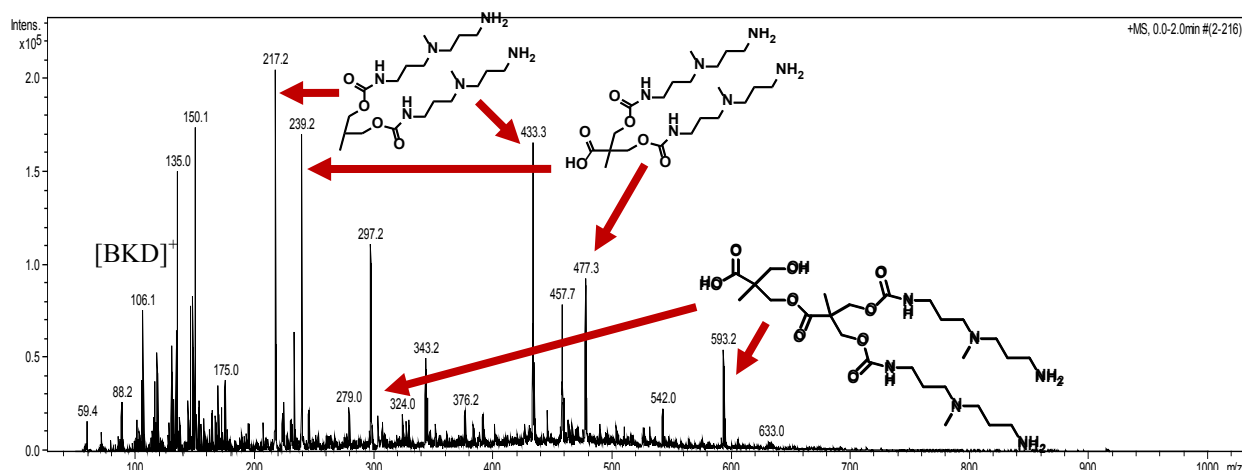


Figure S7. Mass spectra at time = 24 h for **Chol-SS-G2** after stirring at pH 7.5 at 37°C in the presence of DTT (10 mM). The structures of some of the degradation products are illustrated.

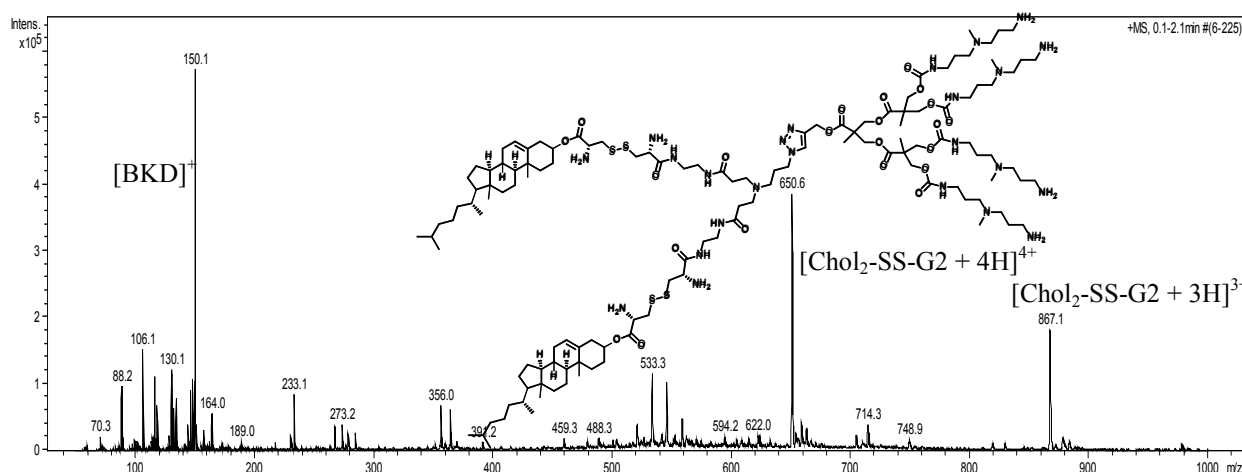


Figure S8. Mass spectra at time = 0 h, for **Chol₂-SS-G1**

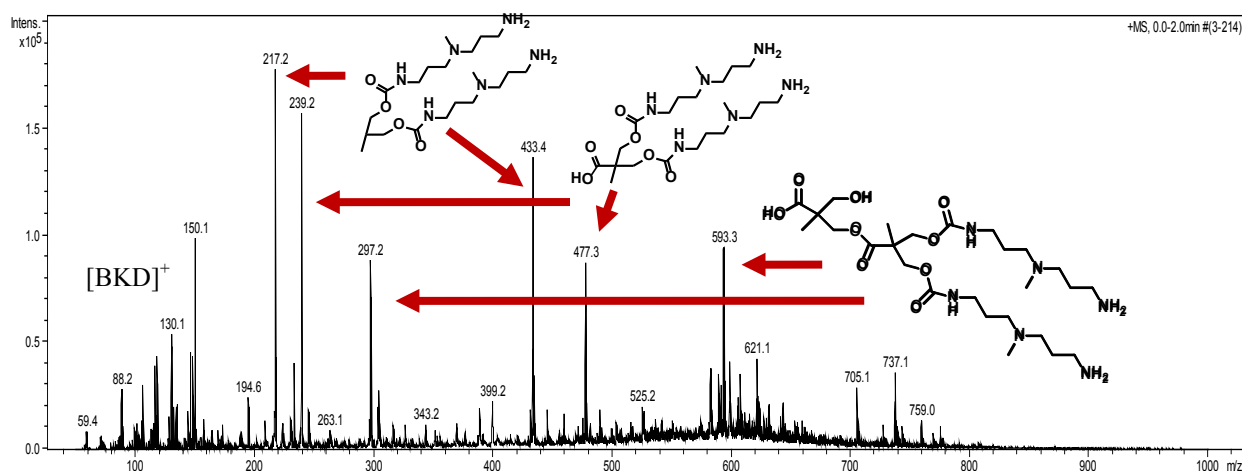


Figure S9. Mass spectra at time = 24 h for **Chol₂-SS-G2** after stirring at pH 7.5 at 37°C. The structure of some of the degradation products are illustrated.

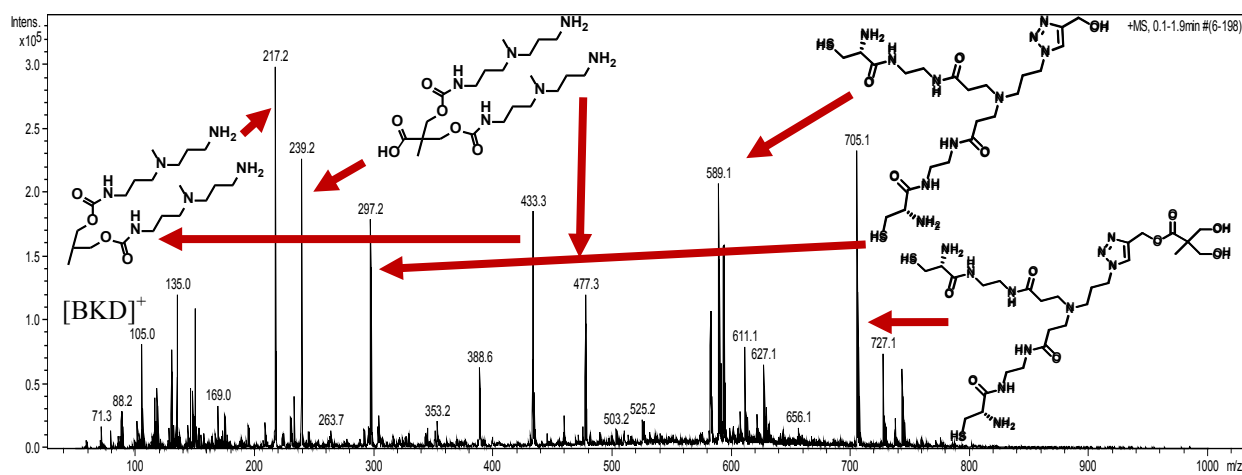


Figure S10. Mass spectra at time = 24 h for **Chol₂-SS-G2** after stirring at pH 7.5 at 37°C in the presence of DTT (10 mM). The structures of some of the degradation products are illustrated.

5 Degradation/DNA Release Assays

5.1 Disulfide Cleavage (Nile Red)

A 2.5 mM Nile Red stock solution was made in EtOH. A dendron stock solution at a concentration above the C.A.C. was made up in PBS buffer (1 ml) and Nile Red (1 μ l) was added followed by DTT with a final concentration of 10 mM. The fluorescence emission was measured at regular time intervals on a Hitachi F-4500 spectrofluorimeter using an excitation wavelength of 550 nm. Fluorescence intensity was recorded at 635 nm. Experiments were performed in triplicate.

5.2 Disulfide Cleavage (Ethidium Bromide)

A stock solution containing Calf Thymus DNA (4.0 μ M with respect to one DNA base), ethidium bromide (5.07 μ M) and either glutathione or dithiothreitol (10 mM) was prepared. This solution was used to prepare a dendron stock solution (1 mg/ml). An appropriate amount of the dendron solution was added to the solution of DNA (4.0 μ M), EthBr (5.07 μ M) and either GSH or DTT (10 mM) to give an N:P of 2. The fluorescence was measured at regular time intervals on a Hitachi F-4500 spectrofluorimeter using an excitation wavelength of 540 nm. Fluorescence intensity was recorded at 595 nm. Background ethidium bromide fluorescence was measured at 5.07 μ M. The fluorescence values were normalised to a solution containing only DNA and ethidium bromide. Experiments were performed in triplicate.

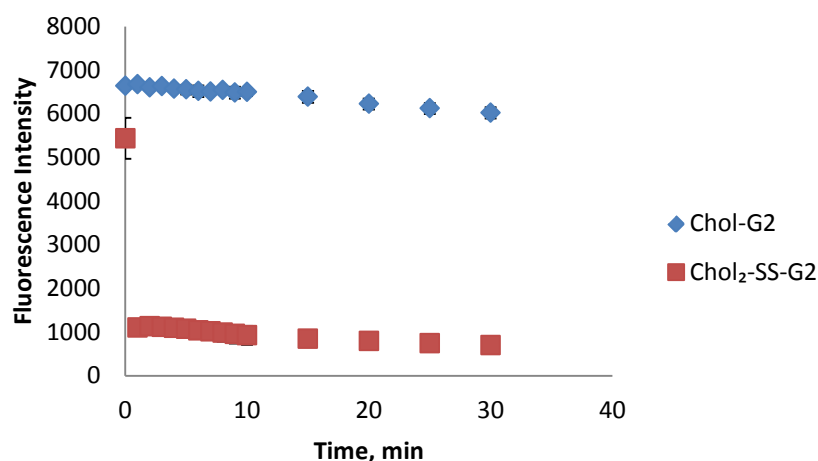


Figure S11. Fluorescence intensity (635 nm) of Nile Red in the presence of **Chol-G2** and **Chol₂-SS-G2** over time on the addition of 10 mM DTT.

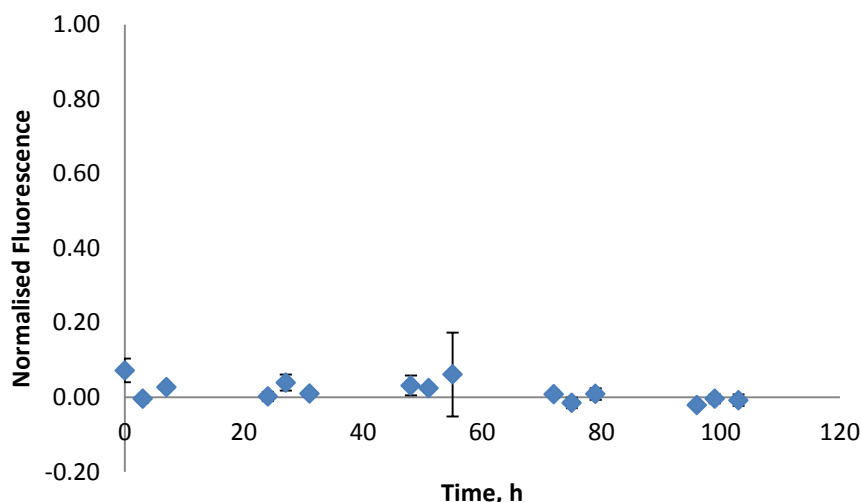


Figure S12. Fluorescence data for **Chol-SS-G2** stirred at 37 °C in the presence of calf thymus DNA (N:P = 2) and ethidium bromide.

6 Multiscale Modelling Methods

In this work, we resorted to our well-validated multiscale molecular modeling procedure^{1,2,5-7} based on systematic elimination of computationally expensive degrees of freedom while retaining implicitly their influence on the remaining degrees freedom in a mesoscopic model. Accordingly, using the information obtained from atomistic molecular dynamics simulation (MD), we parameterized the dissipative particle dynamics (DPD)⁸ models that incorporate all essential physics/phenomena observed at the finer level.

The outline of the general strategy of our multiscale modeling approach may be summarized as follows (for full details *vide infra*): i) explicit solvent atomistic MD calculations were performed on model compounds;⁹ ii) the mesoscale model parameters were calculated exploiting the conformational properties and energetical values obtained from MD simulation at point (i)¹⁰ using an explicit solvent model in which each dendron was represented as single force centers (beads) and solvent was treated explicitly in the presence of ions and counterions. Langevin dynamics were then conducted using the DPD representation of the system; iii) the equilibrium configurations of the self-assembled systems obtained at point (ii) were mapped back to the corresponding atomistic MD models, and then new atomistic MD simulations were conducted to calculate binding energies between each micelle and the DNA molecule.¹

6.1 Atomistic molecular dynamics simulation of dendrons in solution

All atomistic simulations and data analysis were performed with the AMBER 11 suite of programs.¹³ All compound models were built and geometry-optimized using the Antechamber module of AMBER 11 and the GAFF force field.¹⁴ Each dendron structure was then solvated in a TIP3P¹⁵ water box to generate a bulk system with concentration lower than the corresponding experimental CAC value. Then, the required amount of Na⁺ and Cl⁻ ions were added to neutralize the system and to mimic an ionic strength of 150 mM, removing eventual overlapping water molecules. The solvated molecules were subjected to a combination of steepest descent/conjugate gradient minimization of the potential energy, during which all bad contacts were relieved. The relaxed systems were then gradually heated to 300 K in three intervals by running constant volume-constant temperature (NVT) MD simulation, allowing a 0.5 ns interval per each 100 K. Subsequently, 10 ns MD simulations under isobaric-isothermal (NPT) conditions were conducted to fully equilibrate each solvated compound. The *SHAKE* algorithm¹⁶ with a geometrical tolerance of 5×10^{-4} Å was imposed on all covalent bonds involving hydrogen atoms. Temperature control was achieved using the Langevin¹⁷ temperature equilibration scheme and an integration time step of 2 fs. At this point, these MD runs were followed by other 10 ns of NVT MD and 10 ns of NVT data collection runs. The particle mesh Ewald method¹⁸ was used to treat the long-range electrostatics. For the calculation of interaction energies and conformational properties, 1000 snapshots were saved during the MD data collection period described above, one snapshot per each 10 ps of MD simulation.

All of the production molecular dynamics simulations were carried out working in parallel on IBM FERMI and Eurora calculation cluster of the CINECA supercomputer centre (Bologna, Italy).

6.2 Background theory of mesoscopic Dissipative Particle Dynamics (DPD) simulations

DPD is a particle-based mesoscale technique first introduced by Hoogerbrugge and Koelman^{8b} and cast in its present form by Español and Warren,¹⁹ and Groot and Warren.^{8a} In DPD, a number of particles are coarse-grained into fluid elements, called beads. These DPD beads interact via pairwise additive interactions that locally conserve momentum, a necessary condition for a correct description of hydrodynamics, while retaining essential information about the structural and physical-chemical properties of the system components. An advantageous feature of DPD is that it employs soft repulsive interactions between the beads, thereby allowing for larger integration time steps than in a typical molecular dynamics using for example Lennard-Jones interactions. Thus, time and length scales much larger (up to microseconds range) than those in atomistic molecular dynamics simulations can be accessed. In DPD the beads move according to Newton's equations of motion:

$$d\mathbf{r}_i(t) / dt = \mathbf{p}_i(t) / m_i \quad (\text{SI1})$$

$$d\mathbf{p}_i(t) / dt = \mathbf{f}_i(t) \quad (\text{SI2})$$

where $\mathbf{r}_i(t)$, $\mathbf{p}_i(t)$, m_i , and $\mathbf{f}_i(t)$ are the position, momentum, mass and net force of particle i , respectively. $\mathbf{f}_i(t)$ is given as the sum of three different forces: a conservative force $\mathbf{F}_{ij,C}$, a dissipative force $\mathbf{F}_{ij,D}$, and a random force $\mathbf{F}_{ij,R}$:

$$\mathbf{f}_i(t) = \sum_{i \neq j} \mathbf{F}_{ij,C} + \mathbf{F}_{ij,D} + \mathbf{F}_{ij,R} \quad (\text{SI3})$$

All forces are pairwise and lay along the line joining two interacting particles i and j . The conservative force for non-bonded beads $\mathbf{F}_{ij,C}$ represents a soft repulsion modeled as a linear function of the distance between two particles, while the dissipative force $\mathbf{F}_{ij,D}$ slows down the particle motions, thus accounting for the effects of viscosity, and the random force $\mathbf{F}_{ij,R}$ provides the thermal or vibrational energy of the system. The dissipative force acts to reduce the relative momentum between beads i and j , while random force $\mathbf{F}_{ij,R}$ impels energy into the system. The expressions for the forces are given by the following equations:

$$\mathbf{F}_{ij,C} = a_{ij} (1 - r_{ij} / r_c) \times \mathbf{r}_{ij} / r_{ij} \quad (\text{SI4})$$

$$\mathbf{F}_{ij,D} = -\gamma_{ij} \omega^D(r_{ij}) [(\mathbf{r}_{ij} / r_{ij}) \times \mathbf{v}_{ij}] (\mathbf{r}_{ij} / r_{ij}) \quad (\text{SI5})$$

$$\mathbf{F}_{ij,R} = \sigma_{ij} \omega^R(r_{ij}) (\zeta_{ij} / \Delta t^{0.5}) (\mathbf{r}_{ij} / r_{ij}) \quad (\text{SI6})$$

where a_{ij} is the maximum repulsion parameter between particle i and j , $\mathbf{r}_{ij} = \mathbf{r}_i - \mathbf{r}_j$ is the vector joining beads i and j , $r_{ij} = |\mathbf{r}_{ij}|$ is the distance between particle i and j , $\mathbf{v}_{ij} = \mathbf{v}_i - \mathbf{v}_j$ is the relative velocity, and $\mathbf{v}_i = \mathbf{p}_i / m_i$. All the above forces acts within the cut-off radius r_c , which basically constitutes the length scale of the entire system. γ_{ij} is a friction coefficient, σ_{ij} the noise amplitude, ζ_{ij} a Gaussian random number with a zero mean and a unit variance chosen independently for each pair of particles, and Δt is the time step in the simulation. $\omega^D(r_{ij})$ and $\omega^R(r_{ij})$ are weight functions vanishing for distance greater than r_c .

In DPD, molecules are built by tying beads together using Hookean springs with the potential given by:

$$U_{bb}(i, i+1) = \frac{1}{2} k_{bb} (r_{i,i+1} - l_0)^2 \quad (\text{SI7})$$

where $i, i+1$ label adjacent beads in the molecule. The spring constant, k_{bb} , and unstretched length l_0 , are chosen so as to fix the average bond length to a desired value. Chain stiffness is modeled by a three body potential acting between adjacent bead triples in a row using equation (SI8):

$$U_{bbb}(i-1, i, i+1) = k_{bbb} (1 - \cos(\phi - \phi_0)) \quad (\text{SI8})$$

in which the angle ϕ is defined by the scalar product of the two bonds connecting the pair of adjacent beads $i-1$, i , and $i+1$.

Furthermore, in order to correctly derive the electrostatic interactions between charged beads (i.e. present on the dendrons and ions), the electrostatic force F_{ij}^E between two charged beads i and j is analysed following the approach reported in Groot's work.²⁰ According to this study, the electrostatic field is solved by smearing the charges over a lattice grid, the size of which is determined by a balance between the fast implementation and the correct representation of the electrostatic field.

6.3 DPD modeling of dendron self-assembly

We modelled the different compounds at a coarse-grained level using branched and flexible amphiphilic chains made up of 5 bead types: one hydrophilic charged bead H, as the terminal charged repeating unit of the dendron, one hydrophobic building block C, representing the cholesterol moiety, two further bead types, L1 and L2, linking the hydrophilic and hydrophobic parts together, and one beads S for the disulfide linkage.

Comparing the appropriate MD and DPD pair-pair correlation functions, we determined the mesoscale topology of each single dendron molecule.^{1,2,10b,10d,10f,21} The coarse-grained models obtained for each compound are shown in Figure S13.

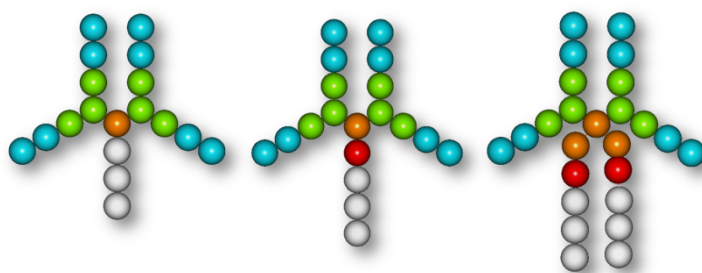


Figure S13. Schematic representation of the coarse-grained DPD models of the three dendrons considered in this work. Left to right: **Chol-G2**, **Chol-SS-G2**, and **Chol₂-SS-G2**. The colours of the beads stand for hydrophilic dendron beads H (light blue), cholesterol tail beads C (white), linker beads L1 (orange) and L2 (acid green), and disulphide linkage moiety S (red).

Solvent molecules were simulated by single bead types *W*, and an appropriate number of counterions of a charge of ± 1 were added to preserve charge neutrality and to account for the experimental solution ionic strength. The inclusion of explicit counterions was necessary because counterion condensation and the interactions between the counterions and the charged groups may affect the complex structure to a certain extent. All simulations were performed in a 3D-periodic cubic box equivalent to a bulk system of volume $35^3 r_c^3$. The appropriate number of dendron molecules was added to the simulation box in order to fit experimental concentrations. Approximately 7×10^6 time steps at 300 K were performed in each DPD run, thus corresponding to a total physical time for each calculation of about 2 μ s.

The intra- and intermolecular interactions between DPD particles are expressed by the conservative parameter a_{ij} , defined by equation (SI4). This quantity accounts for the underlying chemistry of the system considered. In this work, we employed a well-validated strategy that correlates the interaction energies estimated from atomistic molecular dynamics simulations²² to the mesoscale a_{ij} parameter values.^{2,10,23} Following and adapting this computational recipe to the present case, the interaction energies between the solvated dendron molecules estimated using the MD-based procedure described above were rescaled onto the corresponding mesoscale segments. The bead-bead interaction parameter for water was set equal to $a_{ww} = 25$ in agreement with the correct value of DPD density $\rho = 3$.^{8a} The maximum level of hydrophobic/hydrophilic repulsion was captured by setting the interaction parameter a_{ij} between the positively charged dendron bead *H* and the cholesterol tail bead as 80. The counterions were set to have the interaction parameters of water.²⁴ Once these parameters were assigned, all the remaining bead-bead interaction parameters for the DPD simulations were easily obtained, starting from the atomistic interaction energies values, as described in our previous works.^{2,10f} The entire set of DPD interaction parameters employed in this work are summarized in Table S1.

Table S1. DPD bead-bead interaction parameters obtained for the three molecules in water.

a_{ij}	<i>H</i>	<i>L1</i>	<i>L2</i>	<i>C</i>	<i>S</i>	<i>W</i>
<i>H</i>	41	33	32	80	56	21
<i>L1</i>	33	25	31	40	38	33
<i>L2</i>	32	31	25	48	42	32
<i>C</i>	80	40	48	25	51	75
<i>S</i>	56	38	42	51	62	70
<i>W</i>	21	33	32	75	70	25

The analysis of the equilibrated trajectories allows the determination of the relevant system characteristics, such as the self-assembled morphology of the dendrons, aggregation number, micellar dimension, micellar surface charge density etc.

6.4 Atomistic molecular dynamics simulations of dendron micelles/DNA complex

Exploiting the morphological information obtained at the mesoscale level, the corresponding atomistic models of the micelle were built and relaxed in a 150 mM NaCl solution, adopting the same procedure reported above. From the corresponding equilibrated systems, all water molecules and counterions were removed, and a 21base-pair B-DNA chain was placed in complex with the micelle. Each complex was then solvated with an appropriate number of TIP3P¹⁵ water molecules extending at least 30 Å from the solute. A suitable number of Na⁺ and Cl⁻ counterions were added to neutralize the system and to mimic an ionic strength level of 0.15 M. Eventual overlapping water molecules were removed. Each system was then subjected to a combination of steepest descent and conjugate gradient energy minimization steps (50000 cycles), in order to relax close atomic distances, fixing the micelle/DNA complex in their initial configuration using a harmonic constraint with a force constant of 500 kcal/(mol Å²). The optimized systems were then i) gradually heated from 0 to 300 K using MD simulations in the canonical ensemble (NVT), allowing a 1 ns interval per each 100 K with an integration step of 1 fs, and employing a weak harmonic constraint (i.e., 25 (kcal/mol)/Å²) on the solute, and ii) equilibrated for 10 ns at 300 K under *Shake* constraint¹⁶ with a geometric tolerance of 5×10⁻⁴ Å on all covalent bonds involving hydrogen atoms to prevent a substantial disruption of the hydrogen bond network. Further system equilibration was performed by carrying out MD simulations in the isobaric-isothermal (NPT) ensemble. During equilibration, different energetic components as well as static and conformational properties (e.g., radius of gyration of the dendrimer, average distance between the micelle and the nucleic acid, and distribution of ions and water molecules around the complex) were monitored, to ensure their stabilization prior to production runs. 10 ns MD runs were performed on equilibrated systems in the NPT ensemble with 1fs time step (T = 300 K, P = 1 bar). The Langevin method¹⁷ (with a damping coefficient of 5 ps⁻¹) and the Nose-Hoover Langevin piston method²⁵ (using a piston period of 0.8 ps and a decay time of 0.4 ps) were employed for temperature and pressure control, respectively. Electrostatic interactions were computed by means of the particle mesh Ewald (PME) algorithm.¹⁸ At this point, these MD runs were followed by other 10 ns NPT MD simulations during which the force constant of the harmonic constraints were gradually brought to zero in steps of 5 kcal/(mol Å²) each.

Finally, 40 ns of NVT data collection runs, were carried out. For the calculation of the binding free energy between the B-DNA and each micelle, 4000 snapshots were saved during the MD data collection period described above, one snapshot per each 10 ps of MD simulation.

All of the production (MD) simulations were carried out by using AMBER 11 platform and the *ff03* all-atom force field by Duan et al.²⁶ working in parallel on IBM FERMI and Eurora calculation cluster of the CINECA supercomputer center (Bologna, Italy). The DNA fragment was generated using the *Nucleic Acid Builder* feature of *AmberTools 1.5*²⁷. All energetic analyses were performed by running the *MM/PBSA*¹¹ script supplied with AMBER 11 on a single 40 ns MD trajectory of each micelle/DNA complex considered.

For a non-covalent association of two molecular entities $A + B \rightarrow AB$, the free energy of binding involved in the process may be generally written as $\Delta G_{\text{bind}} = G_{\text{AB}} - G_{\text{A}} - G_{\text{B}}$. For any species on the right hand side of this equation, from basic thermodynamics we have $G_i = H_i - TS_i$, where H_i and S_i are the enthalpy and entropy of the i -th species, respectively and T is the absolute temperature. In view of this expression, ΔG_{bind} can then be written as:

$$\Delta G_{\text{bind}} = \Delta H_{\text{bind}} - T\Delta S_{\text{bind}} \quad (\text{SI9})$$

ΔH_{bind} is the variation in enthalpy upon association and, in the MM/PBSA framework of theory, can be calculated by summing the molecular mechanics energies (ΔE_{MM}) and the solvation free energy (ΔG_{solv}), i.e., $\Delta H_{\text{bind}} = \Delta E_{\text{MM}} + \Delta G_{\text{solv}}$. ΔE_{MM} is obtained directly from a single MD trajectory of the molecular complex as $\Delta E_{\text{MM}} = \Delta E_{\text{vdW}} + \Delta E_{\text{ele}}$, where ΔE_{vdW} is the variation of the nonbonded van der Waals energy and ΔE_{ele} is the electrostatic contribution calculated from the Coulomb potential.

The solvation/desolvation contribution to the free energy, ΔG_{solv} , can also be also split in two components:

$$\Delta G_{\text{solv}} = \Delta G_{\text{PB}} + \Delta G_{\text{NP}} \quad (\text{SI10})$$

The calculations of the polar solvation term ΔG_{PB} were done with the *DelPhi* package,²⁸ with interior and exterior dielectric constants equal to 1 and 80, respectively. The dielectric boundary is the contact surface between the radii of the solute and the radius (1.4 Å) of a water molecule. The numerical solution of the linearized Poisson-Boltzmann equations were solved on a cubic lattice by using the iterative finite-difference method implemented in *DelPhi*. A grid spacing of 0.25 Å, extending 50 % beyond the dimensions of the solute, was employed. Potentials at the boundaries of the finite-difference lattice were set to the sum of the Debye-Hückel potentials. The non-polar component ΔG_{NP} was obtained using the following relationship:²⁹

$$\Delta G_{\text{NP}} = \gamma SA + \beta \quad (\text{SI11})$$

in which $\gamma = 0.00542 \text{ kcal}/\text{Å}^2$, $\beta = 0.92 \text{ kcal/mol}$, and the molecular surface area SA was estimated by means of the MSMS software.³⁰

Finally, entropic contributions arising from changes in the molecular degrees of freedom (translational,

rotational, and vibrational) were included applying classical statistical thermodynamics.³¹ Due to the high computational demand, calculations were performed only a subset of 20 snapshots sampled from the equilibrated MD trajectories, and were based on based on a harmonic approximation of the normal mode and standard formulae. Each frame was energy minimized through a series of relaxations that first applied the generalized Born (GB)³² method in AMBER 11 followed by *in vacuum* minimization with a distance-dependent dielectric constant of $\epsilon = 4r$. These steps were further followed by Newton-Raphson minimizations until the root-mean square of the elements of the gradient vector was less than 10^{-4} kcal/mol Å.

Finally, the effective number of charges involved in binding, and the corresponding effective free energy of binding values (Table 5) were obtained performing a *per residue binding free energy decomposition* exploiting the MD trajectory of each given DNA/micelle complex. This analysis was carried out using the MM/GBSA approach³³ and was based on the same snapshots used in the binding free energy calculation.

6.5 Free energy of micellization

From an energetic standpoint, the change in Gibbs free energy of transfer of a single amphiphilic molecule from the monomeric state to a micelle of aggregation number N_{agg} , commonly called the free energy of micellization ΔG_{mic} , can be modeled as consisting of a hydrophobic part, $\Delta G_{mic,h}$, and an electrostatic part, $\Delta G_{mic,e}$, so that $\Delta G_{mic} = \Delta G_{mic,h} + \Delta G_{mic,e}$. The hydrophobic part stems primarily from the favorable energy of transfer of the hydrocarbon moieties from the aqueous phase to the micellar phase, and, secondarily, from the unfavorable residual interfacial contact of water with the apolar components within the micelles. The electrostatic part of ΔG_{mic} arises from the repulsion between the ionic head groups within the micellar shell. We calculated the values of ΔG_{mic} for the three amphiphilic dendrons (Table 2) following the theory proposed by Tanford³⁴ and subsequently modified by other authors.³⁵

6.6 Calculation of zeta potential

We calculated the surface electrostatic potential Ψ_s of the charged dendron micelles according to the formula:³⁶

$$\frac{e\sigma_m}{\kappa\varepsilon_r\varepsilon_0k_B T} = \Psi_s + \frac{\Psi_s}{\kappa r} - \frac{\tau_1^2 \kappa r}{\tau_2 - \tau_1 \kappa r} \quad (\text{SI12})$$

where κ^{-1} is the Debye length, σ_m is the micelle surface charge per unit area, ε_0 is the permittivity of vacuum, ε_r corresponds to the relative permittivity, $k_B T$ is the product of the Boltzmann constant and absolute temperature, e is the elementary charge, and:

$$\tau_1 = 2 \sinh \frac{\Psi_s}{2} - \Psi_s \quad (\text{SI13})$$

$$\tau_2 = 4 \tanh \frac{\Psi_s}{4} - \Psi_s \quad (\text{SI14})$$

Accordingly, the electrostatic potential at the diffuse layer (DL) boundary ζ , known as the zeta potential, was obtained from the Debye-Hückel approximation as:

$$\zeta = \Psi_s \left(\frac{r}{r + \kappa^{-1}} \right) e^{-1} \quad (\text{SI15})$$

where $(r + \kappa^{-1})$ is the distance of DL boundary from the center of mass of the micelle. The Debye parameter κ in Equation (SI12) is obtained from the inverse of Debye length given by:

$$\kappa^{-1} = \sqrt{\frac{\varepsilon_0 \varepsilon_r k_B T}{2 N_A e^2 I}} \quad (\text{SI16})$$

where N_A is Avogadro's number and I is the ionic strength of the solution.

7 References

1. S. P. Jones, N. P. Gabrielson, C.-H. Wong, H.-F. Chow, D. W. Pack, P. Posocco, M. Fermeglia, S. Pricl and D. K. Smith, *Mol Pharm*, 2011, **8**, 416-429.
2. A. Barnard, P. Posocco, S. Pricl, M. Calderon, R. Haag, M. E. Hwang, V. W. T. Shum, D. W. Pack and D. K. Smith, *J. Am. Chem. Soc.* 2011, **133**, 20288-20300.
3. M. C. A. Stuart, J. C. van de Pas and J. B. F. N. Engberts, *J. Phys. Org. Chem.* 2005, **18**, 929-934.
4. (a) B. F. Cain, B. C. Baguley and W. A. Denny, *J. Med. Chem.* **1978**, *21*, 658-668. (b) H. Gershon, R. Ghirlando, S. B. Guttman and A. Minsky, *Biochemistry* 1993, **32**, 7143-7151.
5. P. Posocco, E. Laurini, V. Dal Col, D. Marson, K. Karatasos, M. Fermeglia and S. Pricl, *Curr. Med. Chem.* 2012, **19**, 5062-5087.
6. X. Liu, J. Wu, M. Yammine, J. Zhou, P. Posocco, S. Viel, C. Liu, F. Ziarelli, M. Fermeglia, S. Pricl, G. Victorero, C. Nguyen, P. Erbacher, J. P. Behr and L Peng, *Bioconjugate Chem.* 2011, **22**, 2461-2473.
7. P. Posocco, S. Pricl, S. P. Jones, A. Barnard and D. K. Smith, *Chem. Sci.* 2010, **1**, 393-404.

8. (a) R. D. Groot and P. B. Warren, *J. Chem. Phys.* 1997, **107**, 4423-4435. (b) P. J. Hoogerbrugge and J. M. V. A. Koelman, *EPL (Europhysics Letters)* 1992, **19**, 155-160.
9. (a) X. Liu, C. Liu, E. Laurini, P. Posocco, S. Pricl, F. Qu, P. Rocchi and L. Peng, *Mol. Pharm.* 2012, **9**, 470-481. (b) K. Karatasos, P. Paola, E. Laurini and S. Pricl, *Macromol Biosci.* 2012, **12**, 225-240. (c) G. M. Pavan, P. Paola, A. Tagliabue, M. Maly, A. Malek, A. Danani, E. Ragg, C. V. Catapano and S. Pricl, *Chem. Eur. J.* 2010, **16**, 7781-7795. (d) S. P. Jones, G. M. Pavan, A. Danani, S. Pricl and D. K. Smith, *Chem. Eur. J.* 2010, **16**, 4519-3245. (e) G. M. Pavan, A. Danani, S. Pricl, D. K. Smith, *J. Am. Chem. Soc.* 2009, **131**, 9686-9694.
10. (a) P. Posocco, C. Gentilini, S. Bidoggia, A. Pace, P. Franchi, M. Lucarini, M. Fermeglia, S. Pricl and L. Pasquato, *ACS Nano* 2012, **6**, 7243-7253. (b) R. Toth, F. Santese, S. P. Pereira, D. R. Nieto, S. Pricl, M. Fermeglia and P. Posocco, *J. Mater. Chem.* 2012, **22**, 5398-5409. (c) P. Posocco, Z. Posel, M. Fermeglia, M. Lisal and S. Pricl, *J. Mater. Chem.* 2010, **20**, 10511-10520. (d) G. Scocchi, P. Posocco, J. W. Handgraaf, J. G. Fraaije, M. Fermeglia and S. Pricl, *Chem. Eur. J.* 2009, **15**, 7586-7592. (e) M. Maly, P. Posocco, S. Pricl and M. Fermeglia, *Ind. Eng. Chem. Res.* 2008, **47**, 5023-5038. (f) G. Scocchi, P. Posocco, M. Fermeglia and S. Pricl, *J. Phys. Chem. B* 2007, **111**, 2143-2151.
- 11 J. Srinivasan, T. E. Cheatham, P. Cieplak, P. A. Kollman and D. A. Case, *J. Am. Chem. Soc.* 1998, **120**, 9401-9409.
- 12 P. Posocco, M. Ferrone, M. Fermeglia and S. Pricl, *Macromolecules* 2007, **40**, 2257-2266.
13. D. A. Case, T. A. Darden, T. E. Cheatham III, C. L. Simmerling, J. Wang, R. E. Duke, R. Luo, R. C. Walker, W. Zhang, K. M. Merz, B. Roberts, B. Wang, S. Hayik, A. Roitberg, G. Seabra, I. Kolossváry, K. F. Wong, F. Paesani, J. Vanicek, X. Wu, S. R. Brozell, T. Steinbrecher, H. Gohlke, Q. Cai, X. Ye, J. Wang, M.-J. Hsieh, G. Cui, D. R. Roe, D. H. Mathews, M. G. Seetin, C. Sagui, V. Babin, T. Luchko, S. Gusarov, A. Kovalenko and P. A. Kollman AMBER 11, 2010, University of California, San Francisco, CA, USA.
14. (a) J. Wang, R. M. Wolf, J. Caldwell, P. A. Kollman and D. A. Case, *J. Comput. Chem.* 2004, **25**, 1157-1174. (b) J. Wang, P. A. Kollman and D. A. Case, *J. Mol. Graph. Model.* 2006, **25**, 247-260.
15. W. L. Jorgensen, J. Chandrasekhar, J. D. Madura, R. W. Impey and M. L. Klein, *J. Chem. Phys.* 1983, **79**, 926-935.
16. J.-P. Ryckaert, G. Ciccotti and H. J. C. Berendsen, *J. Comput. Phys.* 1977, **23**, 327-341.
17. R. J. Loncharich, B. R. Brooks and R. W. Pastor, *Biopolymers* 1992, **32**, 523-535.
18. A. Toukmaji, C. Sagui, J. Board and T. Darden, *J. Chem. Phys.* 2000, **113**, 10913-10927.
19. P. Español and P. Warren, *Europhys. Lett.* 1995, **30**, 191-196.
20. R. D. Groot *J. Chem. Phys.* 2003, **118**, 11265-11277.
21. (a) P. Posocco, M. Fermeglia and S. Pricl, *J. Mater. Chem.* 2010, **20**, 7742-7753. (b) M. Fermeglia and S. Pricl, *Comput. Chem. Eng.* 2009, **33**, 1701-1710. (c) R. Toth, D.-J. Voorn, J.-W. Handgraaf, J.

- G. E. M. Fraaije, M. Fermeglia, S. Pricl and P. Posocco, *Macromolecules* 2009, **42**, 8260-8270. (d)
G. Scocchi, P. Posocco, A. Danani, S. Pricl and M. Fermeglia, *Fluid Phase Equilibria* 2007, **261**, 366-374.
22. (a) M. Fermeglia, M. Ferrone and S. Pricl, *Fluid Phase Equilib.* 2003, **212**, 315–329. (b) R. Toth, A. Coslanich, M. Ferrone, M. Fermeglia, S. Pricl, S. Miertus and E. Chiellini, *Polymer* 2004, **45**, 8075–8083. (c) M. Fermeglia, M. Ferrone and S. Pricl, *Mol. Simul.* 2004, **30**, 289–300.
23. D. J. Welsh, P. Posocco, S. Pricl and D. K. Smith, *Org. Biomol. Chem.* 2013, **11**, 3177-3186.
24. X. Fan, N. Phan-Thien, S. Chen, X. Wu, T. Y. Ng, *Phys. Fluids* 2006, **18**, 63102-63110.
25. S. E. Feller, Y. Zhang, R. W. Pastor and B. R. Brooks, *J. Chem. Phys.* 1995, **103**, 4613-4621.
26. Y. Duan, C. Wu, S. Chowdhury, M. C. Lee, G. M. Xiong, W. Zhang, R. Yang, P. Cieplak, R. Luo, T. Lee, J. Caldwell, J. Wang and P. Kollman, *J. Comput. Chem.*, 2003, **24**, 1999–2012.
27. D. A. Case, D. T. Darden, T. E. Cheatham, C. L. Simmerling, J. Wang, R. E. Duke, R. Luo, R. C. Walker, W. Zhang, K. M. Merz, B. Roberts, B. Wang, S. Hayik, A. Roitberg, G. Seabra, I. Kolossváry, K. F. Wong, F. Paesani, J. Vanicek, J. Liu, X. Wu, S.R. Brozell, T. Steinbrecher, H. Gohlke, Q. Cai, X. Ye, J. Wang, M. J. Hsieh, G. Cui, D. R. Roe, D. H. Mathews, M. G. Seetin, C. Sagui, V. Babin, T., S. Gusarov, A. Kovalenko, and P. A. Kollman, University of California, San Francisco., 2010.
28. M. K. Gilson, K. A. Sharp and B. H. Honig, *J. Comput. Chem.* 1988, **9**, 327-335.
29. D. Sitkoff, K. A. Sharp and B. H. Honing., *J. Phys. Chem.* 1994, **98**, 1978-1988.
30. M. F. Sanner, A. J. Olson and J.-C. Spehner, *Biopolymers* 1996, **38**, 305-320.
31. I. Andricioaei and M. Karplus, *J. Chem. Phys.* 2001, **115**, 6289-6292.
32. M. S. Lee, M. Feig, F. R. Jr Salsbury and C.L Brooks, *J. Chem. Phys.* 2002, **116**, 10606-10614.
33. (a) V. Tsui and D. A. Case, *Biopolymers* 2000, **56**, 275-291. (b) A. Onufriev, D. Bashford and D. A. Case, *J. Chem. Phys. B* 2000, **104**, 3712-3720.
34. C. Tanford, *Krieger Publishing Co.*, Malabar, FL, 1991, pp. 60.
35. (a) C. S. Patrickios, *J. Phys. Chem.* 1995, **99**, 17437-17441. (b) R. Nagarajan, *Langmuir* 2002, **18**, 31-38.
36. J. E. Sader, *Coll. Interface Sci.* 1997, **188**, 508-510.